JOURNAL OF AGRICULTURAL AND FOOD CHEMISTRY

Article

pubs.acs.org/JAFC

Adsorption Characteristics of (−)-Epigallocatechin Gallate and Caffeine in the Extract of Waste Tea on Macroporous Adsorption Resins Functionalized with Chloromethyl, Amino, and Phenylamino Groups

Yongfeng Liu,[†,§] Qingqing Bai,[†,⊥] Song Lou,[†,§] Duolong Di,*[,†,‡] Jintian Li,[⊥] and Mei Guo[⊥]

[†]Key Laboratory of Chemistry of Northwestern Plant Resources and Key Laboratory for Natural Medicine of Gansu Province, Lanzhou Institute of Chemical Physics, Chinese Academy of Sciences, No. 18, Tianshui Middle Road, Lanzhou 730000, China

[‡]Center of Resource Chemical and New Material, Lanzhou Institute of Chemical Physics, Chinese Academy of Sciences, No.36, Jinshui Road, Qingdao 266100, China

[§]Graduate University of the Chinese Academy of Sciences, No. 19A, Yuquan Road, Beijing 100049, China

[⊥]Department of Pharmacy, Gansu College of Traditional Chinese Medicine, No. 35, Dingxi East Road, Lanzhou 730000, China

ABSTRACT: According to the Friedel−Crafts and amination reaction, a series of macroporous adsorption resins (MARs) with novel structures were synthesized and identified by the Brunauer−Emmett−Teller (BET) method and Fourier transform infrared (FTIR) spectra, and corresponding adsorption behaviors for (−)-epigallocatechin gallate (EGCG) and caffeine (CAF) extracted from waste tea were systemically investigated. Based on evaluation of adsorption kinetics, the kinetic data were well fitted by pseudo-second-order kinetics. Langmuir, Freundlich, Temkin−Pyzhev, and Dubinin−Radushkevich isotherms were selected to illustrate the adsorption process of EGCG and CAF on the MARs. Thermodynamic parameters were adopted to explain in-depth information of inherent energetic changes associated with the adsorption process. The effect of temperature on EGCG and CAF adsorption by D101-3 was further expounded. Van der Waals force, hydrogen bonding, and electrostatic interaction were the main driving forces for the adsorption of EGCG and CAF on the MARs. This study might provide a scientific reference point to aid the industrial large-scale separation and enrichment of EGCG from the extracts of waste tea using modified MARs.

KEYWORDS: *(−)-Epigallocatechin gallate, caffeine, waste tea, macroporous adsorption resin, adsorption isotherm, adsorption kinetics*

INTRODUCTION

It is well known that tea, mainly steeped from the leaves of *Camellia sinensis* L., which is native to China, is one of the most widely consumed beverages in the world. According to statistics, the tea production in China has reached 1.1 million tons annually. In recent years, tea deep processing has been quickly developed, and many kinds of tea products now appear in the market. Consequently, the quantity of waste tea has been increasing year by year. Waste tea not only pollutes the environment but also represents a loss of valuable resources. Waste tea residues contain abundant tea polyphenols and caffeine (CAF), which are rich in medical value. Tea polyphenols comprise various compounds, such as (−)-epigallocatechin gallate (EGCG), (−)-epigallocatechin (EGC), (−)-epicatechin gallate (ECG), and (−)-epicatechin (EC), which are the major bioactive components in many functional beverages and foods. EGCG is probably the most powerful antioxidant among them. The chemical structures of EGCG and CAF are shown in Figure 1.

Research clearly indicates that EGCG has many biological activities, including anticancer and anti-inflammatory effects,[1] strong antimicrobial activity,[2,3] antiviral effects,[4] preventing HIV-1 infection,[5] growth inhibition of prostate cancer cells,[6] inhibitory effects on mutations,[7] and modulation of cholesterol metabolism.[8] Moreover, dietary supplementation with EGCG significantly reduces the development of obesity, hyperglycemia, insulin resistance, hypercholesterolemia, and hepatic steatosis.[9] Hence, EGCG is extensively employed in the fields of medication, beverages, and foodstuffs. As an important component of tea, CAF increases endurance and enhances performance, increases neuromuscular coordination, enhances cognitive functioning, elevates mood, and relieves anxiety.[10−13] However, excessive intake of CAF may inevitably cause adverse effects, such as sleep deprivation, increased risk of cardiovas-

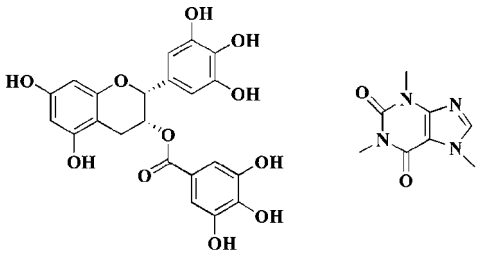

Figure 1. Chemical structures of (−)-epigallocatechin gallate (EGCG) and caffeine (CAF).

Received: November 17, 2011
Revised: January 9, 2012
Accepted: January 13, 2012
Published: January 13, 2012

dx.doi.org/10.1021/jf204710h | *J. Agric. Food Chem.* 2012, 60, 1555−1566

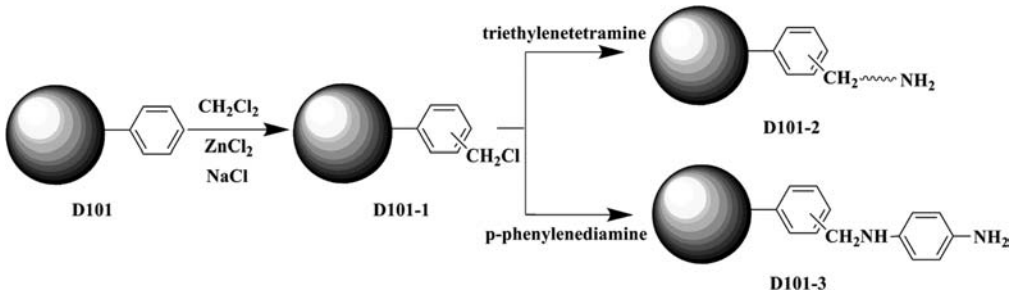

Figure 2. Reaction scheme for the preparation of D101-1, D101-2, and D101-3 on the basis of D101.

cular disease and miscarriages, reduced fertility rates, and increased seizure frequency and aggravated seizures.[14,15] Therefore, it is necessary to develop an efficient method to obtain highly enriched EGCG and, as far as possible, to decrease the content of CAF prior to application in pharmaceuticals, functional foods, and beverages.[16]

Because of the important effect of EGCG on humans and the significance of decaffeinated tea extracts, several approaches for the separation and purification of EGCG and CAF have been attempted and extensively reported in many previous studies. The common methods of decaffeination are as follows: extraction with organic solvent such as chloroform or methylene chloride and ethyl acetate with potential unsafe effects from the residual organic solvents,[17] supercritical fluid extraction with expensive equipment and unavoidably large amount of catechins loss results,[18,19] and hot water treatment, which is only suitable for producing low-caffeine or decaffeinated green tea.[20] Methods for microgram degradation and for genetically modified caffeine-free tea plants have been developed.[21−23] However, these methods have not yet reached industrial scale production because of technology limitations. Activated carbon, tea stalk, lignocellulose, and fir sawdust lignocellulose grafted with *N*-vinylpyrrolidone adsorbents have been established for separating decaffeinated catechins.[16,24−26] Recently, poly(acrylamide-co-ethylene glycol dimethacrylate) and poly(vinylpolypyrrolidone) have been used for separating decaffeined catechins.[27,28] Therefore, the method of adsorption using an adsorbent has attracted widespread attention.

Because of the advantages of high efficiency, simple operation process, low operation cost, easy regeneration, long lifetime, and being environmentally friendly, macroporous adsorption resins (MARs) are widely employed as alternative and effective adsorbents in separating bioactive components from crude extracts of herbal raw materials.[29−33] In recent years, many researchers have also developed adsorption theories for MARs.[34,35] Because the functional group of the adsorbent is one of the most important key factors for improving separation efficiency, scientists have made great efforts to explore novel, desirable adsorbents with special functional groups that possess high adsorption capacity and perfect selectivity.[36−38] Therefore, MARs modified by special functional groups have a high potential for applications in the separation and purification fields to obtain bioactive components from crude extracts of natural products.

In this study, a series of MARs with special functional groups were synthesized based on the Friedel−Crafts and amination reaction and identified by the Brunauer−Emmett−Teller (BET) method and Fourier transform infrared (FTIR) spectra. Adsorption kinetics and thermodynamics of the MARs for EGCG and CAF extracted from waste tea were systemically investigated through static adsorption tests, and the effect of temperature on EGCG and CAF adsorption by MARs was further studied. The experimental data were fitted by the common models of kinetics and thermodynamics. The results might provide a scientific reference point for the industrial-scale separation and enrichment of active ingredients from the extracts of natural products using MARs that possess special functional groups.

MATERIALS AND METHODS

Chemical Reagents, Adsorbents, and Samples. Chromatographic grade methanol and acetic acid were purchased from Shandong Yuwang Industrial Co., Ltd. (Shandong, China), and distilled water was used. D101, nonpolar styrene-co-divinylbenzene copolymer with no functional groups, was purchased from Xi'an Sunresin Technology Co., Ltd. (Shaanxi, China). Waste tea (production area: Longnan) was obtained from a local market in Longnan City (Gansu Province, China). The standard EGCG was purchased from Chengdu Purifa Technology Development Co., Inc. (Sichuan, China), and the purity was 99.0%. The standard CAF was isolated and purified from the extract of waste tea in our laboratory, and the purity was determined as more than 95.0% by HPLC analysis based on the peak area normalization method.

Synthesis of Adsorbents with Functional Groups. The reaction scheme for the preparation of D101-1, D101-2, and D101-3 on the basis of D101 is shown in Figure 2. The initial MARs (D101) were soaked in dichloromethane for 24 h. An organic solution composed of dichloromethane, zinc chloride initiator, sodium chloride, and D101 was mixed with chloromethyl methyl ether in a 1000 mL three-necked round-bottomed flask equipped with a mechanical stirrer, a reflux condenser, and a thermometer. The flask was heated with a programmed heater. The mixture was stirred to give a suspension of beads of a suitable size in the solution (100−120 rpm) and then held at 323.15 K for 20 h. The synthetic MARs were filtered out, packed in an extractor, and washed with a large amount of distilled water and then methanol until there was no white precipitate while an aqueous solution of silver nitrate was added to the filtrate. The MARs with chloromethyl groups (D101-1) were obtained. The MARs with amino groups were synthesized through an amination reaction. The D101-1 were dried at 313.15 K under vacuum, swelled with methanol for 24 h, and mixed with excess triethylenetetramine in a 500 mL three-necked round-bottomed flask. The mixture was held at 303.15 K for 9 h. Then the beads were filtered out and washed with distilled water until there was no white precipitate while an aqueous solution of silver nitrate was added to the filtrate. MARs with amino groups (D101-2) were obtained. MARs with phenylamino groups (D101-3) were

synthesized using a method similar to that of the amination reaction.

Characterization of MARs. The BET specific surface area, average pore size, and pore volume of the adsorbents were determined by N_2 adsorption/desorption isotherms at 77.15 K using a Micromeritics ASAP 2020 automatic surface area and porosity analyzer (Micromeritics Instrument Corp., Norcross, GA) by the BET method. The MARs were outgassed for 24 h with the temperature at 333 K on the degas port of the analyzer before the measurement of BET surface area. The BET surface area was obtained by the *t*-plot method. Meanwhile, the pore volume and average pore diameter were estimated by the Barrett–Joyner–Halenda (BJH) method. FTIR spectra of MARs were obtained on a FTIR spectrophotometer (Thermo Nicolet, NEXUS, TM) in the 4000–400 cm^{-1} region via the KBr pellet method, and FTIR spectra (the FTIR spectra were not shown) showed that chloromethyl, amino, and phenylamino groups had been successfully introduced on D101.[35]

Preparation of Tea Extract and Sample Solutions. Waste tea (1 kg) was refluxed with 8 L of ethanol–water (60:40, v/v) solution for 30 min in triplicate. All of the extracts were mixed, filtrated by gauze, and evaporated to a fluid extract by removing the solvent under reduced pressure in a rotary evaporator at 323.15 K. The extracts obtained were placed in a vacuum drying oven and dried at 313.15 K until the mass was constant. Then the dried extracts were ground to powder and stored in refrigerator at 277.15 K. EGCG and CAF contents in the dried extract were 13.0% and 7.3% (w/w), respectively. Distilled water was added to obtain sample solutions of different concentrations.

HPLC Analysis of EGCG and CAF. The HPLC analysis was performed in an Agilent 1200 Series (Agilent Technology, Santa Clara, CA), which was equipped with a G1312A binary pump, a G1315B diode array detector and a G1328B manual injector. The HPLC system was managed by Agilent Chemstation software (version A.10.02) (Agilent Technology). The standards EGCG and CAF were accurately weighed and dissolved in distilled water to produce the stock standard solutions with the concentrations of 1.6 and 0.9 mg/mL, respectively. The chromatographic separation of analytes was performed on a SinoChrom ODS-BP C_{18} analytical column (250 mm × 4.6 mm, i.d., 5 μm) (Dalian Elite Analytical Instruments Co. Ltd., Dalian, China). The temperature of the column was maintained at 318.15 K. Chromatographic separation was performed using a gradient elution with methanol (A) and 1% acetic acid in water (B). The mobile phase gradient was as follows: 85–70% (B) at 0–5 min, 70% (B) at 5–15 min, 70–62% (B) at 15–25 min, and 62% (B) at 25–35 min. The flow rate, injection volume, and detection wavelength were set at 1.0 mL/min, 20 μL, and 280 nm, respectively. The wavelength of DAD detector ranged from 200 to 400 nm. The HPLC results demonstrated that the working calibration curve showed excellent linearity over the range of 0.00102–1.56 mg/mL and 0.00058–0.92 mg/mL, respectively. The regression lines for EGCG and CAF were $y = 22822x - 208.8$ ($R^2 = 0.9980$, $n = 7$) and $y = 39653x - 4.3$ ($R^2 = 0.9990$, $n = 7$), respectively, where y is the peak area of EGCG or CAF, and x is EGCG or CAF concentration (mg/mL).

Calculation of Adsorption Capacity. The adsorption capacities of the MARs toward EGCG and CAF were evaluated according to the following equation.

Adsorption capacity is given as:

$$q_e = (C_0 - C_e) \times \frac{V_0}{W}$$

where q_e is the adsorption capacity (mg/g dry resin) toward EGCG or CAF at adsorption equilibrium. C_0 and C_e are the initial and equilibrium concentrations of EGCG or CAF solutions (mg/mL). W is the weight of resin used (g).

In addition, the adsorption studies mentioned below were conducted in triplicate, and the deviation error was less than 5%. On the basis of the results of preliminary study, desorption performance of EGCG and CAF on the selected MARs with ethanol–water (70:30, v/v) as an eluent was efficient, and the MARs used were almost completely recovered in 30 min.

Adsorption Kinetics. The adsorption kinetics curves of EGCG and CAF on the MARs were studied according to the following operation mode: 200 mL of extract solution (C_0 = 2.0 mg/mL) was contacted with pretreated MARs (1.0 g dry resin) in a 500 mL stoppered conical flask. Then the flasks were continually shaken in SHA-B incubator (100 rpm) (Jintan Zhengji Instrument Co., Ltd., Jiangsu Province, China) at 298.15, 308.15, and 318.15 K, respectively. Subsequently, the concentration of EGCG and CAF in the adsorption solution was determined by HPLC at different times until equilibrium.

Adsorption Isotherm. Extract solutions (50 mL) with different concentrations of EGCG and CAF (C_0 = 2.0, 4.0, 6.0, 8.0, 10.0, and 12.0 mg/mL) were contacted with pretreated MARs (1.0 g of dry resin) in conical flasks. The flasks were continually shaken for 8 h at temperatures of 298.15, 308.15, and 318.15 K, respectively. Then, the EGCG and CAF concentrations of the adsorption solutions were analyzed by HPLC.

Effect of Temperature of EGCG and CAF on D101-3. The experiment was carried out by adding 1.0 g of pretreated D101-3 resin and 50 mL of 12.0 mg/mL tea extracts to each flask with a lid, and the flasks were continually shaken for 8 h at the temperatures of 298.15 K, 308.15 K, 318.15 K, 328.15 K, 338.15 K, and 348.15 K, accordingly. The concentrations of EGCG and CAF in the adsorption solutions were determined by HPLC.

RESULTS AND DISCUSSION

Characterization of the MARs. Nitrogen adsorption/desorption measurements were performed with the MARs before and after modification with functional groups. The adsorption/desorption isotherms of D101, D101-1, D101-2, and D101-3 are shown in Figure 3. The isotherms of D101, D101-1, D101-2, and D101-3 were similar, and these MARs were mainly mesoporous according to the IUPAC nomenclature. In addition, it was clear that the order of pore volume of these MARs (D101-1 > D101 > D101-3 > D101-2) was in line with those depicted in Figure 3.

Physical properties of D101, D101-1, D101-2, and D101-3 were determined from nitrogen adsorption/desorption isotherms using *t*-plot and BJH methods and are tabulated in Table 1. As shown in Table 1, BET surface areas followed an order of D101 > D101-1 > D101-3 > D101-2. This order indicated that BET surface areas of MARs decreased after modification with functional groups. And the reason was that the MARs swelled in the process of the reaction. The average pore diameters of MARs were in the order of D101-1 > D101-2 > D101-3 > D101, as shown in Table 1, which was also ascribed to the swelling of MARs in the reaction process. The pore

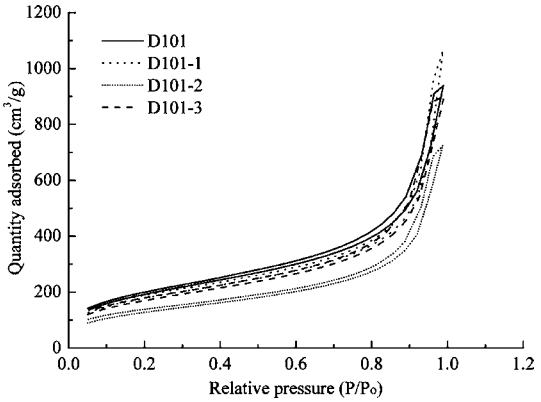

Figure 3. Nitrogen adsorption/desorption isotherms of D101, D101-1, D101-2, and D101-3.

Table 1. Physical Properties of D101, D101-1, D101-2, and D101-3

resin series	D101	D101-1	D101-2	D101-3
matrix	P(St-DVB)	P(St-DVB)	P(St-DVB)	P(St-DVB)
functional group		chloromethyl	amino	phenylamino
BET surface area (m^2/g)	710.1	656.0	471.4	626.4
average pore diameter (nm)	8.2	10.0	9.5	8.9
pore volume (cm^3/g)	1.5	1.6	1.1	1.4
particle size (mm)	0.2−0.3	0.2−0.3	0.2−0.3	0.2−0.3

volumes of MARs were in the order of D101-1 > D101 > D101-3 > D101-2 in Table 1. The small pore volume of D101-2 might be due to a cross-linking reaction that took place in the synthetic process as triethylenetetramine was added into reaction vessel.

Fractal geometry, widely used in many fields of modern science, is also popularly applied in adsorption science. The fractal dimension D, an operative measure of the surface and structural irregularities of a given solid, is the key quantity in fractal geometry. Several isotherm equations have been derived for various models of physical adsorption on fractal surfaces to calculate D. Based on the Frenkel−Halsey−Hill (FHH) equation, one of simplest and most popular relationships in logarithmic form to determine D of a solid is estimated as follows:[39,40]

$$\ln q = \text{const} - (3 - D)\ln A$$

where q (cm^3/g) is the amount of N_2 adsorbed at the relative pressure p/p_0, and D is the fractal dimension of the surface accessible to adsorption. A is the so-called adsorption potential, defined as:

$$A = RT \ln(p_0/p)$$

where p_0 and p are the saturation and equilibrium vapor pressures (mmHg), R is the universal gas constant (8.314 J/(mol K)), and T is the absolute temperature (K).

A plot of ln q versus ln A showed a linear trend, and D was calculated from the slope. The values of D for D101, D101-1, D101-2, and D101-3 were 2.64, 2.62, 2.61, and 2.63, respectively. On the basis of the theory of fractal geometry, the value of the fractal dimension D for solid surfaces can vary from 2 to 3. It is reported that the lower limiting value of 2 corresponds to a perfectly regular smooth surface, whereas the upper limiting value of 3 relates to the maximum allowed complexity of the surface.[41] The values of the fractal dimension D of MARs followed an order of D101 > D101-3 > D101-1 > D101-2. This demonstrated that the values of D of MARs decreased after modification by functional groups, which meant that the surface of modified MARs became relatively regular smooth. On the other hand, the values of D of D101, D101-1, D101-2, and D101-3 slightly changed, and their degrees of regular smooth almost remained constant. This might be because the amount of functional groups was less and similar.[35]

Adsorption Kinetics of EGCG and CAF on the MARs. The evaluation of kinetics is necessary for the process of purification of EGCG and CAF. It is helpful for the prediction of important information, such as adsorption time and sample concentration. Adsorption kinetics of EGCG and CAF on the MARs was studied at 298.15 K, 308.15 K, and 318.15 K, respectively. The adsorption kinetics curves were obtained, as shown in Figure 4. Figure 4A shows that the adsorption capacity for EGCG on D101 increased with the extension of adsorption time until equilibrium. Generally, the adsorption capacity rapidly increased in the first 40 min and then slowly increased. Finally, the adsorption capacity reached equilibrium after 240 min. This result indicated that the adsorption of EGCG on D101 pertained to the slow adsorption type.[32] In addition, the adsorption capacity for EGCG on D101 decreased with the increase in the temperature. In Figure 4B and 4C, the adsorption capacities for EGCG on D101-1 and D101-2 had a similar increase trend. In Figure 4E, the adsorption capacity for CAF on D101 also displayed this similar trend. However, the adsorption capacity reached equilibrium after 180 min, which indicated that the adsorption of CAF on D101 pertained to the intermediate speed adsorption type.[32] The adsorption capacity for CAF on D101 alike decreased with the increase in temperature. The adsorption kinetics curves in Figure 4F and 4G were similar to those in Figure 4E.

The equilibrium time of EGCG on D101, D101-1, and D101-2 was longer than that of CAF, on the basis of the molecular structures of EGCG and CAF. As shown in Figure 1, obviously, the molecular size of EGCG was much larger than that of CAF. Compared with CAF, high intraparticle mass transfer resistance existed in the process of EGCG diffusion into the mesoporous/micropores of D101, D101-1, and D101-2.

The adsorption behaviors of EGCG and CAF on D101-3 were different from those on D101, D101-1, and D101-2. In Figure 4D, the adsorption capacity for EGCG on D101-3 rapidly increased in the first 20 min. Thereafter it proceeded at a slower rate from 20 to 240 min. Finally, the adsorption capacity increased very slowly after 240 min. Therefore, the adsorption of EGCG on D101-3 belongs to the slow adsorption type.[32] More importantly, the adsorption capacity for EGCG on D101-3 increased with the increase in the temperature. However, the adsorption behavior of CAF on D101-3 was remarkable. In Figure 4H, the adsorption capacity for CAF on D101-3 rapidly increased in the first 20 min. Then it increased slowly from 20 to 180 min. Finally, the adsorption process reached equilibrium after 180 min. Thus, it showed that the adsorption of CAF on D101-3 was the intermediate speed adsorption type.[32] Furthermore, the adsorption capacity of CAF on D101-3 changed slightly at 298.15 K, 308.15 K, and

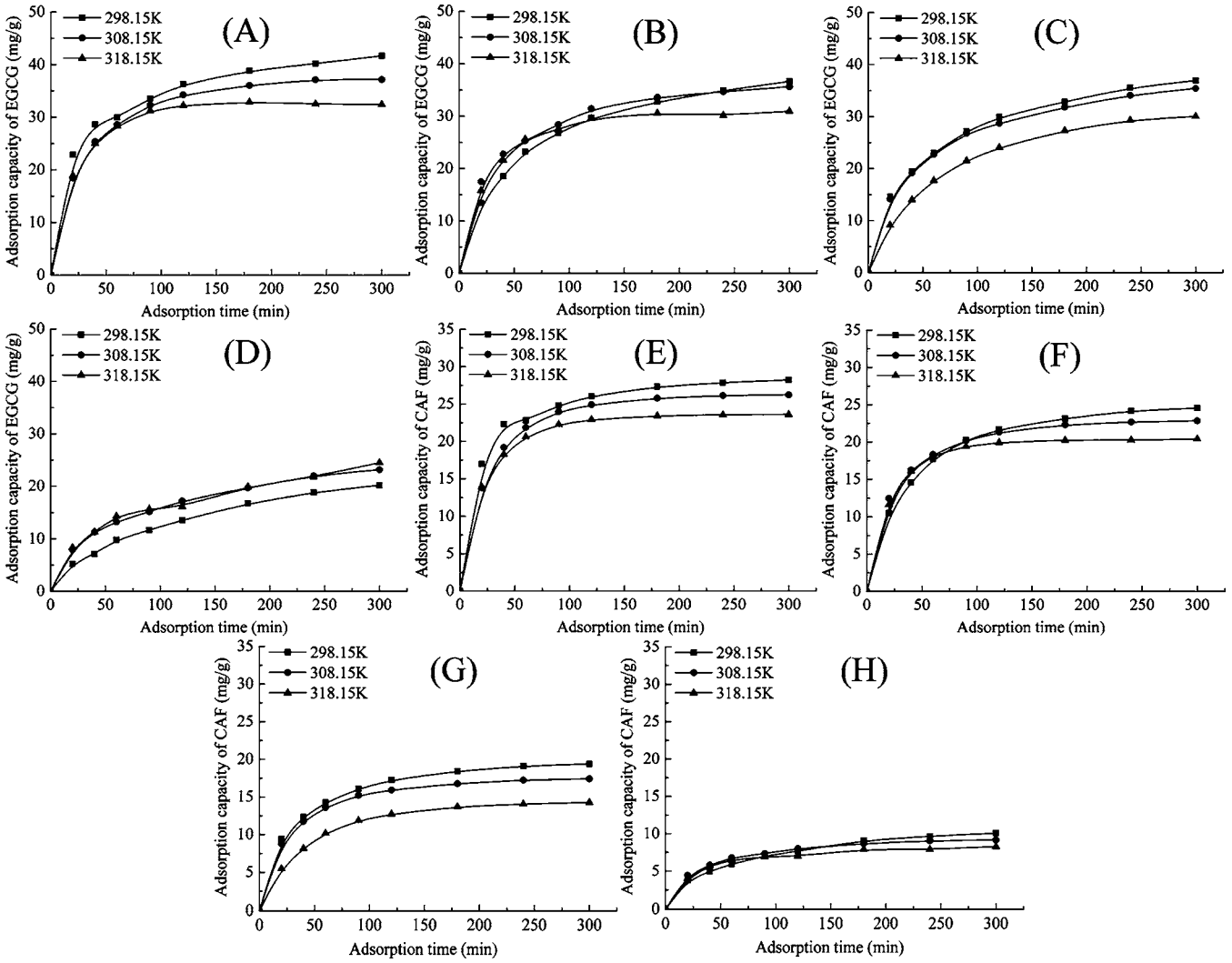

Figure 4. Adsorption kinetics curves of (−)-epigallocatechin gallate (EGCG) (A–D) and caffeine (CAF) (E–H) on D101, D101-1, D101-2, and D101-3 at different temperatures.

318.15 K, and it decreased with the increase in the temperature. Therefore, the purification of EGCG from the extract of waste tea under the conditions of higher temperature and sufficient adsorption time is potentially possible.

To better illustrate the adsorption mechanisms of EGCG and CAF onto the MARs, pseudo-second-order and pseudo-first-order kinetics models were applied. The best-fit model was selected on the basis of the linear regression correlation coefficient values (R^2). The pseudo-second-order and pseudo-first-order kinetics equations are presented as follows.

Equation of pseudo-first-order kinetics model:

$$\ln(q_e - q_t) = \ln q_e - k_1 t$$

Equation of pseudo-second-order kinetics model:

$$\frac{t}{q_t} = \frac{1}{k_2 q_e^2} + \frac{1}{q_e} t$$

where q_e and q_t are the adsorption capacity for EGCG or CAF onto the MARs at equilibrium and at any time t (mg/g dry resin), respectively. The parameters k_1 (1/min) and k_2 (g/(mg min)) are the rate constants of the pseudo-first-order and pseudo-second-order models for the adsorption process, respectively.

Plotting $\ln(q_e - q_t)$ against t for the pseudo-first-order equation and t/q_t against t for the pseudo-second-order equation resulted in straight lines, respectively. Corresponding values of kinetic parameters are summarized in Table 2. Compared with experimental results, the values of q_e and R^2 for the pseudo-second-order model were much more reasonable than those for the pseudo-first-order model. Moreover, most of the q_e values of the pseudo-first-order model deviated significantly from the experimental values. Thus, the adsorption of EGCG and CAF onto the MARs fitted the pseudo-second-order model best, and this model was applied for the entire adsorption process. Further, the principle of pseudo-second-order kinetics assumed that the rate-limiting step might be the adsorption, in agreement with chemical adsorption being the rate-controlling step, in which concentrations of both adsorbate and adsorbent were involved. That is to say, the adsorption of EGCG and CAF onto the MARs might be chemical adsorption or chemisorption.[42] The adsorption process of EGCG and CAF onto the MARs might involve valence forces through sharing or exchange of electrons between EGCG or CAF and the adsorbents. The adsorption force between EGCG or CAF and D101 or D101-1 might be $\pi-\pi$ or electrostatic interaction of the heteroatom and the phenyl rings of the MARs. However,

dx.doi.org/10.1021/jf204710h | J. Agric. Food Chem. 2012, 60, 1555–1566

Table 2. Values of Kinetic Parameters for Adsorption of EGCG and CAF from the Sample Solution Using the MARs

		pseudo-first-order equation			pseudo-second-order equation		
kinetic model		k_1 (1/min)	q_e (mg/g)	R^2	k_2 (g/mg min)	q_e (mg/g)	R^2
298.15 K	EGCG						
	D101	0.011	22.3	0.9964	0.00089	44.6	0.9982
	D101-1	0.011	28.2	0.9969	0.00048	42.2	0.9988
	D101-2	0.012	29.2	0.9853	0.00051	42.2	0.9977
	D101-3	0.011	20.4	0.9789	0.00036	26.7	0.9856
	CAF						
	D101	0.015	13.0	0.9911	0.0021	29.7	0.9997
	D101-1	0.016	18.8	0.9893	0.0011	27.3	0.9998
	D101-2	0.016	13.5	0.9953	0.0017	21.2	0.9998
	D101-3	0.013	8.8	0.9882	0.0015	11.8	0.9947
308.15 K	EGCG						
	D101	0.025	41.8	0.9089	0.0011	40.4	0.9997
	D101-1	0.013	22.7	0.9971	0.00088	38.9	0.9991
	D101-2	0.012	26.9	0.9898	0.00057	40.2	0.9984
	D101-3	0.011	20.0	0.9687	0.00059	27.4	0.9916
	CAF						
	D101	0.021	17.1	0.9942	0.0021	28.0	0.9994
	D101-1	0.018	14.1	0.9993	0.0021	24.4	0.9998
	D101-2	0.017	11.2	0.9932	0.0024	18.8	0.9999
	D101-3	0.016	6.8	0.9819	0.0034	10.1	0.9994
318.15 K	EGCG						
	D101	0.012	8.4	0.7172	0.0025	34.2	0.9983
	D101-1	0.016	14.4	0.7973	0.0016	33.0	0.9987
	D101-2	0.015	30.3	0.9827	0.00044	36.5	0.9995
	D101-3	0.0077	18.2	0.9782	0.00055	28.1	0.9749
	CAF						
	D101	0.024	13.9	0.9962	0.0032	24.8	0.9994
	D101-1	0.020	7.8	0.9020	0.0040	21.4	0.9990
	D101-2	0.017	11.7	0.9990	0.0017	16.2	0.9988
	D101-3	0.011	4.1	0.9059	0.0046	8.8	0.9982

besides forces mentioned above, hydrogen-bonding interaction existed between EGCG or CAF and D101-2 or D101-3.

Adsorption Isotherms of EGCG and CAF on the MARs. Before synthesis of MARs with functional groups, the initial MARs (D101) were soaked in dichloromethane for 24 h in order to swell sufficiently. MARs used in the experiment had swelled enough. On the other hand, distilled water and ethanol, with swelling ability comparatively weaker than that of dichloromethane, were applied in the adsorption/desorption process. Furthermore, the volumes of the MARs after adsorption had almost no change compared with those before adsorption. In this case, the factor of swelling of the MARs was ignored in the study.

The equilibrium adsorption isotherms of EGCG and CAF from aqueous solution onto the MARs were obtained at 298.15 K, 308.15 K, and 318.15 K, respectively, as shown in Figure 5. It was obvious that the adsorption capacities for EGCG and CAF onto D101 increased with an increase in the equilibrium concentration of EGCG and CAF at the given temperature in Figure 5A and 5E. Generally, the adsorption capacity for EGCG increased rapidly when the concentration of EGCG was less than 0.05 mg/mL and then increased slowly above 0.05 mg/mL. However, the adsorption capacity for CAF increased rapidly at a nearly constant rate when the concentration of CAF increased. Furthermore, the adsorption capacities for EGCG and CAF onto D101 decreased with an increase in the experimental temperature, which might suggest an exothermic process. A similar result was obtained for D101-1 and D101-2 as illustrated in Figure 5B, 5F, 5C, and 5G.

However, the equilibrium adsorption isotherms of EGCG and CAF onto D101-3 were not in accordance with that of D101, D101-1, and D101-2, and possessed special characteristics. As shown in Figure 5D, the adsorption capacity for EGCG onto D101-3 increased rapidly when the concentration of EGCG was less than 0.05 mg/mL and then increased slowly above 0.05 mg/mL. However, the rate increased with the increase in experimental temperature when the concentration of EGCG was more than 0.05 mg/mL. In addition, the adsorption capacities for EGCG onto D101-3 increased with an increase in the experimental temperature, which might suggest an endothermic process.[43,44] The adsorption capacity for CAF onto D101-3 increased rapidly with a nearly constant rate when the concentration of CAF increased. The adsorption isotherms at the three temperatures almost overlapped with each other in Figure 5H. The difference in adsorption characteristics for EGCG and CAF onto D101-3 was exceedingly helpful to purify EGCG from the extract of waste tea using MARs.

In general, the adsorption isotherm is the functional expression of the relationship between the equilibrium concentration of an adsorbate in solution and the amount of solid adsorbent at a given temperature under adsorption equilibrium conditions. Thus, through fitting experimental data, the optimized isotherm can be obtained by comparing the values of correlation coefficients. Further, it is helpful to understand the adsorption mechanism of the adsorbate onto

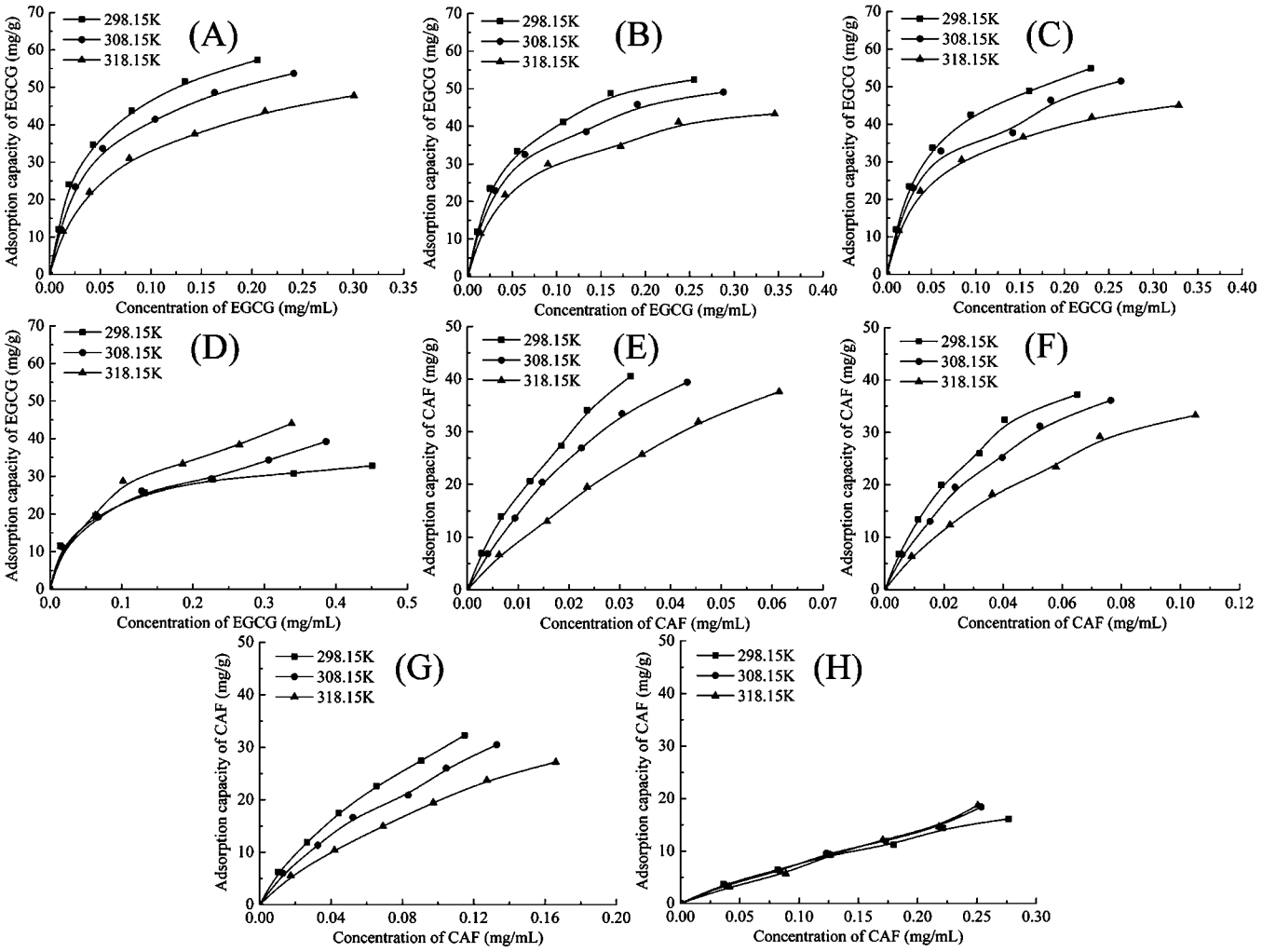

Figure 5. Adsorption isotherms of (−)-epigallocatechin gallate (EGCG) (A−D) and caffeine (CAF) (E−H) on D101, D101-1, D101-2, and D101-3 at different temperatures.

Table 3. Langmuir Isotherm Parameters for the Adsorption Process of EGCG and CAF onto MARs at 298.15 K, 308.15 K, and 318.15 K

		EGCG				CAF			
isotherm parameters		q_m (mg/g)	K_L (mg/mL)	r_L^2	R_L	q_m (mg/g)	K_L (mg/mL)	r_L^2	R_L
D101	298.15 K	69.7	0.042	0.9906	0.026	62.9	0.023	0.9970	0.025
	308.15 K	60.3	0.042	0.9992	0.025	75.2	0.040	0.9989	0.044
	318.15 K	50.1	0.045	0.9936	0.028	67.7	0.058	0.9917	0.062
D101-1	298.15 K	60.5	0.043	0.9975	0.027	55.2	0.034	0.9982	0.037
	308.15 K	52.2	0.038	0.9972	0.024	50.9	0.039	0.9933	0.043
	318.15 K	45.3	0.042	0.9949	0.026	50.7	0.063	0.9966	0.067
D101-2	298.15 K	63.8	0.045	0.9995	0.028	44.0	0.063	0.9910	0.067
	308.15 K	55.0	0.042	0.9949	0.026	43.5	0.083	0.9916	0.086
	318.15 K	47.7	0.042	0.9976	0.026	42.5	0.12	0.9929	0.12
D101-3	298.15 K	31.3	0.025	0.9662	0.016	26.6	0.23	0.9873	0.21
	308.15 K	35.8	0.041	0.9582	0.026	37.1	0.36	0.9799	0.29
	318.15 K	42.2	0.049	0.9581	0.031	98.3	1.26	0.9854	0.59

the adsorbent. Many isotherm equations have been proposed to explain the process of adsorption equilibrium. However, several models cannot acquire ideal correlation coefficients in fitting the experimental data. The most widely used isotherm models are Langmuir, Freundlich, Temkin−Pyzhev, and Dubinin−Radushkevich isotherms. In the present investigation, the experimental data were tested with these isotherms.

The Langmuir isotherm model was originally developed to describe chemisorption on a group of localized adsorption sites with the same adsorption energy, independent of the surface coverage and with no interaction between adsorbed molecules.[45] Furthermore, the Langmuir adsorption isotherm assumes that adsorption takes place at specific homogeneous sites within the adsorbent, and all the adsorption sites are

dx.doi.org/10.1021/jf204710h | J. Agric. Food Chem. 2012, 60, 1555−1566

Table 4. Freundlich Isotherm Parameters for the Adsorption Process of EGCG and CAF onto MARs at 298.15 K, 308.15 K, and 318.15 K

isotherm parameters		EGCG			CAF		
		K_F ((mg/g)(mL/mg)$^{1/n}$)	$1/n$	r_F^2	K_F ((mg/g)(mL/mg)$^{1/n}$)	$1/n$	r_F^2
D101	298.15 K	136.7	0.47	0.9346	493.2	0.72	0.9971
	308.15 K	114.3	0.46	0.9521	447.1	0.75	0.9913
	318.15 K	88.7	0.45	0.9761	343.5	0.78	0.9957
D101-1	298.15 K	110.7	0.46	0.9432	252.4	0.66	0.9826
	308.15 K	92.3	0.43	0.9558	217.8	0.67	0.9894
	318.15 K	72.9	0.41	0.9641	167.9	0.69	0.9914
D101-2	298.15 K	122.7	0.48	0.9501	142.6	0.68	0.9992
	308.15 K	97.7	0.44	0.9473	123.5	0.70	0.9963
	318.15 K	78.0	0.42	0.9605	101.5	0.72	0.9987
D101-3	298.15 K	44.2	0.31	0.9785	41.4	0.73	0.9947
	308.15 K	55.9	0.40	0.9917	54.0	0.84	0.9867
	318.15 K	72.9	0.46	0.9839	67.6	0.97	0.9870

energetically identical. It has been used successfully for many adsorption processes of monolayer solid−liquid adsorption.

The Langmuir isotherm equation is represented as:

$$C_e/q_e = K_L/q_m + C_e/q_m$$

where q_e and q_m are the equilibrium and maximum adsorption capacity (mg/g dry resin), respectively. C_e is the equilibrium concentration of EGCG or CAF solution (mg/mL). K_L is the parameter related to the adsorption energy (mg/mL).

Plotting C_e/q_e against C_e resulted in a straight line, and the values of the corresponding parameters were calculated from the intercept and slope. As shown in Table 3, the r_L^2 values were all higher than 0.99 for D101, D101-1, and D101-2, which indicated a very good mathematical fit. The Langmuir isotherm equation reasonably demonstrated the adsorption process of EGCG and CAF. However, the r_L^2 values were lower than 0.99 for D101-3, indicating that an error existed, as the Langmuir isotherm equation was used to explain the adsorption process of EGCG and CAF onto D101-3.

The adsorption mechanism of EGCG and CAF on the MARs was manifested by the Langmuir isotherm theory. Consequently, the essential characteristics of the Langmuir isotherm were represented according to a dimensionless constant, called the separation factor or equilibrium parameter (R_L).[46]

The R_L was given as:

$$R_L = \frac{1}{1 + C_0/K_L}$$

where C_0 is the highest initial concentration of EGCG or CAF (mg/mL), and K_L is the same as mentioned above. The value of R_L gives an indication of the shape of isotherm to be either unfavorable ($R_L > 1$), linear ($R_L = 1$), favorable ($0 < R_L < 1$), or irreversible ($R_L = 0$). In the present study, it was obvious, as shown in Table 3, that the R_L values were all in the range of $0 < R_L < 1$ at different temperatures and MARs. Therefore, it was favorable for the adsorption of EGCG or CAF on the MARs.

The Freundlich isotherm equation, known as an empirical formula, is derived to model the multilayer and heterogeneous surface adsorption. The Freundlich isotherm usually fits the experimental data over a wide range of concentrations and gives the relationship between equilibrium concentration of adsorbate and adsorption capacity of adsorbent.

The Freundlich isotherm equation is shown as:

$$\lg q_e = (1/n)\lg C_e + \lg K_F$$

where K_F reflects the adsorption capacity of an adsorbent ((mg/g)(mL/mg)$^{1/n}$). The parameter n represents the adsorption affinity of the adsorbent for an adsorbate. The parameters q_e and C_e are the same as mentioned above.

According to Freundlich isotherm equation, the plot of lg q_e versus lg C_e using the equilibrium adsorption data would give a straight line, and K_F and $1/n$ were obtained from the intercept and the slope of this straight line, respectively. The values of corresponding parameters are tabulated in Table 4. Regression analysis showed that the Freundlich isotherm was also a good model for EGCG or CAF adsorption on the MARs. Comparison of the r_F^2 values given in Table 4 showed that the experimental data of CAF adsorption on the MARs fitted better than that of EGCG, which meant that the adsorption of CAF and EGCG onto the MARs was a multiple and monolayer layer adsorption, respectively. The reason for this phenomenon was attributed to the molecular size of EGCG and CAF. The molecular structures of EGCG and CAF are shown in Figure 1, and obviously the molecular size of EGCG was much larger than that of CAF. The steric resistance increased with the increase in molecular size, which was a disadvantage for multiple-layer adsorption. In other words, the smaller the molecular size, the easier the multiple-layer adsorption. The values of K_F corresponded to the amount of EGCG or CAF adsorbed onto the MARs. The values of K_F had the same trend as the experimental adsorption capacities for EGCG and CAF. The value of $1/n$ was a measure of adsorption intensity or surface heterogeneity. The value of $1/n$ below 1 demonstrated favorable adsorption, and above 1 was indicative of cooperative adsorption. In the present work, the values of $1/n$ were in the range of 0−1, which indicated that the adsorption of EGCG and CAF onto the MARs was favorable.

The Temkin−Pyzhev isotherm was first developed by Temkin and Pyzhev and describes the behavior of an adsorption system on a heterogeneous surface. It is in accordance with the assumption that the heat of adsorption of all the molecules in the layer decreases linearly with coverage due to adsorbate−adsorbate interactions, and adsorption is characterized by a uniform distribution of binding energies, up to some maximum binding energy.[47]

Table 5. Temkin−Pyzhev Isotherm Parameters for the Adsorption Process of EGCG and CAF onto MARs at 298.15 K, 308.15 K, and 318.15 K

isotherm parameters		EGCG			CAF		
		b_T (J/mol)	A (mL/mg)	r_T^2	b_T (J/mol)	A (mL/mg)	r_T^2
D101	298.15 K	173.1	268.2	0.9991	182.6	479.8	0.9345
	308.15 K	194.8	240.6	0.9985	183.5	336.8	0.9618
	318.15 K	225.8	185.0	0.9942	192.9	208.4	0.9350
D101-1	298.15 K	192.0	240.8	0.9958	207.4	316.4	0.9666
	308.15 K	222.2	246.6	0.9930	218.9	247.7	0.9592
	318.15 K	262.2	212.8	0.9908	236.3	162.4	0.9568
D101-2	298.15 K	179.3	223.5	0.9990	232.8	141.3	0.9415
	308.15 K	202.4	217.1	0.9992	249.1	112.0	0.9313
	318.15 K	252.3	222.8	0.9992	273.7	83.7	0.9436
D101-3	298.15 K	396.2	421.0	0.9929	406.9	42.0	0.9268
	308.15 K	182.2	53.2	0.9599	324.3	8.9	0.9028
	318.15 K	243.6	133.1	0.9552	324.2	28.8	0.8777

Table 6. Dubinin−Radushkevich Isotherm Parameters for the Adsorption Process of EGCG and CAF onto MARs at 298.15 K, 308.15 K, and 318.15 K

isotherm parameters		EGCG				CAF			
		q_m (mg/g)	β ($\times 10^{-8}$ mol^2/J^2)	$r_{D\text{-}R}^2$	E (kJ/mol)	q_m (mg/g)	β ($\times 10^{-8}$ mol^2/J^2)	$r_{D\text{-}R}^2$	E (kJ/mol)
D101	298.15 K	68.8	1.7	0.9917	5.4	59.4	2.0	0.9863	5.0
	308.15 K	58.9	1.6	0.9975	5.5	57.3	2.2	0.9927	4.8
	318.15 K	49.5	1.7	0.9889	5.5	48.7	2.5	0.9702	4.5
D101-1	298.15 K	58.2	1.8	0.9959	5.3	46.9	2.3	0.9899	4.7
	308.15 K	52.0	1.6	0.9940	5.6	42.9	2.4	0.9790	4.6
	318.15 K	44.6	1.6	0.9886	5.6	37.5	2.7	0.9739	4.3
D101-2	298.15 K	61.2	1.8	0.9987	5.2	34.0	3.2	0.9555	3.9
	308.15 K	53.6	1.7	0.9821	5.5	31.3	3.5	0.9477	3.8
	318.15 K	46.8	1.6	0.9946	5.6	27.7	3.9	0.9428	3.6
D101-3	298.15 K	32.0	1.4	0.9685	6.0	15.3	7.2	0.9023	2.6
	308.15 K	44.4	3.2	0.9684	3.9	14.9	33.1	0.8349	1.2
	318.15 K	42.2	1.8	0.9360	5.2	17.7	8.7	0.8836	2.4

The Temkin−Pyzhev isotherm equation is represented as follows:

$$q_e = (RT/b_T)\ln C_e + (RT/b_T)\ln A$$

where R is the gas constant (8.314 J/(mol K)), T is the absolute temperature (K), and A and b_T are the isotherm constant (mL/mg) and Temkin−Pyzhev constant (J/mol), respectively. The parameter q_e is the same as mentioned above.

Based on Temkin−Pyzhev isotherm equation, the values of corresponding parameters obtained from the plot of q_e versus ln C_e are given in Table 5. The correlation coefficients of EGCG onto the MARs were higher than those of CAF, indicating that the isotherm model was more suitable for the EGCG/MARs system than for the CAF/MARs system. The magnitude of adsorption heats (b_T) demonstrated that the adsorption of EGCG and CAF from aqueous solution by the MARs was feasible, indicating a strong affinity of the MARs for EGCG and CAF.

The Dubinin−Radushkevich isotherm represents that the adsorption takes place on a single type of uniform pores, which is analogous to the Langmuir isotherm. It does not suppose a homogeneous surface or constant adsorption potential. Therefore, the Dubinin−Radushkevich isotherm is relatively more common and always applied to distinguish between the physical and chemical adsorption.

The Dubinin−Radushkevich isotherm equation is described as follows:

$$\ln q_e = -\beta\varepsilon^2 + \ln q_m$$

where β is a constant related to the mean free energy of adsorption per mole of an adsorbate (mol^2/J^2) and ε is the Polanyi potential, equal to $RT\ln(1 + 1/C_e)$. R, T, C_e, q_e, and q_m are the same as mentioned above.

The isotherm constants q_m and β were calculated from the slope and intercept of the plot of ln q_e versus ε^2 and are presented in Table 6. As observed from the Table 6, the values of the correlation coefficient for EGCG/MARs and CAF/MARs systems were almost larger than 0.90. Therefore, the experimental data were well fitted by the Dubinin−Radushkevich isotherm.

Further, the constant β gives an idea about the mean free energy E (kJ/mol) of adsorption per molecule of an adsorbate, when the adsorbate is transferred to the surface of the solid adsorbent from the solution. The parameter E was calculated using the relationship given as:

$$E = 1/\sqrt{2\beta}$$

The magnitude of E is a useful parameter for estimating the type of adsorption process, whether the adsorption mechanism is ion-exchange or physical adsorption. The adsorption process might be physical adsorption when E is in the range of 1−8 kJ/

dx.doi.org/10.1021/jf204710h | J. Agric. Food Chem. 2012, 60, 1555−1566

Table 7. Thermodynamics Parameters for the Adsorption Process of EGCG and CAF onto MARs at Different Temperatures

thermodynamics parameters		ΔG^0 (kJ/mol) 298.15 K	308.15 K	318.15 K	ΔH^0 (kJ/mol)	ΔS^0 (J/(mol K))
EGCG	D101	−23.1	−23.9	−24.4	−2.8	68.1
	D101-1	−23.0	−24.1	−24.6	0.6	79.5
	D101-2	−22.9	−23.8	−24.6	2.7	86.0
	D101-3	−24.3	−23.9	−24.2	−27.0	−9.4
CAF	D101	−22.4	−21.7	−21.5	−37.1	−49.2
	D101-1	−21.5	−21.8	−21.2	−24.8	−10.7
	D101-2	−19.9	−19.9	−19.6	−24.7	−15.9
	D101-3	−16.7	−16.1	−13.3	−66.7	−166.6

mol, and ion exchange adsorption when E is between 8 and 16 kJ/mol.[48] As shown in Table 6, the values of adsorption energy, E, for the adsorption of EGCG and CAF on the MARs were found to be in the range of 1−8 kJ/mol at experimental temperatures. Accordingly, it was possible to say that the simple physical adsorption dominated the adsorption process of EGCG and CAF on the MARs due to weak van der Waals forces.

Adsorption Thermodynamics of EGCG and CAF on the MARs. The change in adsorption capacities of EGCG and CAF on the MARs with a rise in temperature was attributed to the exothermic/endothermic nature of the adsorption process. However, it needed to be further explained through evaluation of the thermodynamic parameters, which could provide in-depth information on inherent energetic changes associated with the adsorption process.

The Langmuir isotherm equilibrium constant, K_L, dependent on temperature, can be used to examine thermodynamic parameters. The equilibrium constant K (L/mol) is concerned with the constant K_L. The free energy of adsorption (ΔG^0) is related to the equilibrium constant. Enthalpy (ΔH^0) and entropy (ΔS^0) changes are calculated based on the Van't Hoff equation. Consequently, thermodynamic parameters such as ΔG^0, ΔH^0, and ΔS^0 associated with the adsorption process can be estimated using the following equations:

$$K = M/K_L$$

$$\Delta G^0 = -RT \ln K$$

$$\ln K = -\Delta H^0/RT + \Delta S^0/R$$

where M is the molecular weight of RA or ST (g/mol) and T is the absolute temperature (K). The plot of ln K versus $1/T$ gave a straight line, and the values of ΔH^0 and ΔS^0 were calculated from the slope and intercept, respectively. The corresponding values of ΔG^0, ΔH^0, and ΔS^0 are presented in Table 7.

As shown in Table 7, the ΔG^0 values of the adsorption processes of EGCG and CAF onto the MARs were negative at the investigated temperatures, which indicated that the adsorption processes were spontaneous. The absolute values of ΔG^0 of the adsorption processes of EGCG were larger than that of CAF on corresponding MARs, meaning that the adsorption of EGCG was more advantageous than that of CAF. The ΔH^0 for the adsorption of EGCG on D101-1 and D101-2 was positive, indicating that the process was endothermic in nature, while for the adsorption of EGCG on D101 and D101-3, the opposite result was obtained. The negative values of ΔH^0 for the adsorption of CAF on the MARs indicated that the adsorption processes were exothermic. The positive ΔS^0 values for EGCG on D101, D101-1, and D101-2 implied increasing randomness at the solid−liquid interface during the adsorption process.[49] The reasons were summarized in the following two aspects: First, the values of D (the fractal dimension) of D101, D101-1, and D101-2 were 2.64, 2.62, and 2.61, respectively, which meant that the surfaces of D101, D101-1, and D101-2 were comparatively irregular. Second, the extract of waste tea had many chemical compositions. The adsorbates on the surface of D101, D101-1, and D101-2 also had many kinds of chemical compositions and were irregularly arranged. In addition, the hydrated EGCG would dehydrate once being adsorbed, and then the amount of free water molecules would increase. The randomness of the system depends on the adsorbate and solution. The coordination of dehydration of hydrated EGCG and solution results in the positive entropy. On the contrary, the negative ΔS^0 values for EGCG on D101-3 and CAF on D101, D101-1, D101-2, and D101-3 implied decreasing randomness because the adsorbate molecules were arranged from the irregular state to the regular state at the solid−liquid interface during the adsorption process.

Effect of Temperature on EGCG and CAF Adsorption by D101-3. According to the study of adsorption kinetics, isotherm, and thermodynamics of EGCG/MARs and CAF/MARs systems, the effect of temperature on EGCG and CAF adsorption by D101-3 was further investigated. Figure 6 shows

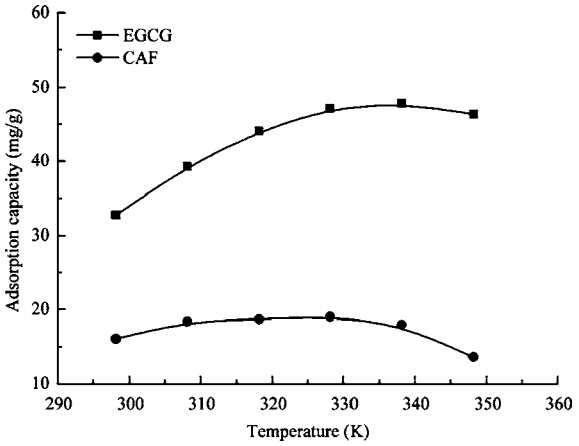

Figure 6. Effect of temperatures on adsorption capacity of (−)-epigallocatechin gallate (EGCG) and caffeine (CAF) on D101-3.

that the adsorption capacity of D101-3 for EGCG increased fast from 298.15 K to 338.15 K, and decreased slightly after 338.15 K. Moreover, adsorption capacity of D101-3 for CAF increased fast from 298.15 K to 308.15 K and then hardly changed from 308.15 K to 328.15 K but decreased quickly after 328.15 K. It was possible that the shape of the EGCG molecule might

relatively match with the pore structure of D101-3 resin at 328.15 K. On the other hand, the mobility of EGCG in the solution was enhanced with the increase in temperature. In general, physisorption was considered to be important for temperatures lower than 373.15 K and chemisorption for temperatures higher than 373.15 K.[50] The experimental temperatures in this study were all lower than 373.15 K, and the mechanism was physical adsorption, validated by the values of *E*. Meanwhile, the stability of EGCG at high temperature should be considered. Therefore, in order to improve adsorption capacity for EGCG and reduce that for CAF, the optimal temperature was 338.15 K for the purification of EGCG from the tea extracts.

Adsorption Mechanisms of EGCG and CAF on the MARs. In general, the adsorbate−adsorbent interaction does play an important role in the adsorption process. The effective interactions include van der Waals force, hydrogen bonding, hydrophobic interaction, and electrostatic interaction. On the basis of the analyses mentioned above, adsorption mechanisms of EGCG and CAF on the MARs were deduced. As shown in Figure 1, EGCG possesses phenyl, hydroxy, and ester groups, and CAF is an N-containing fused heterocycle system with two carbonyl groups. For D101, a nonpolar styrene-co-divinylbenzene copolymer with no functional groups, $\pi-\pi$ interaction between the phenyl rings of D101 and EGCG was one of the main driving forces for the adsorption. Moreover, charge transfer interaction between the phenyl rings of D101 and oxygen atom of EGCG was also an important force. The adsorption of CAF on D101 was similar to that of EGCG. Compared with D101, D101-1 possessed a chloromethyl group, which had hardly any effect on the adsorption of EGCG and CAF. However, by introducing a chloromethyl group into D101, the steric resistance increased so that adsorption capacities for EGCG and CAF slightly decreased. Hydrogen bonding between EGCG and D101-2, with an amino group, was larger than that of CAF and D101-2. Thus, adsorption capacity for EGCG on D101-2 slightly increased, and adsorption capacity for CAF on D101-2 obviously decreased. The adsorption selectivity of EGCG and CAF from the extract of waste tea on D101-3, with a phenylamino group, was increased greatly. This was due to the presence of more $\pi-\pi$ interactions and the formation of more hydrogen bonds between D101-3 and EGCG. That is to say, the affinity of D101-3 for EGCG was much larger than that for CAF. Therefore, on the basis of its selectivity, D101-3 would be most effective for the industrial production of highly enriched EGCG.

AUTHOR INFORMATION

Corresponding Author

*Tel.: +86-931-496-8248; Fax: +86-931-827-7088. E-mail: didl@licp.cas.cn (D.L. Di).

ACKNOWLEDGMENTS

This research project was financially supported by the National Natural Sciences Foundation of China (NSFC No. 20974116) and the "Hundred Talents Program" of the Chinese Academy of Sciences (CAS).

REFERENCES

(1) Lambert, J. D.; Sang, S.; Hong, J.; Yang, C. S. Anticancer and Anti-inflammatory Effects of Cysteine Metabolites of the Green Tea Polyphenol, (−)-Epigallocatechin-3-gallate. *J. Agric. Food. Chem.* **2010**, *58* (18), 10016−10019.

(2) Chacko, S.; Thambi, P.; Kuttan, R.; Nishigaki, I. Beneficial effects of green tea: A literature review. *Chin. Med.* **2010**, *5* (1), 1−9.

(3) Sun, L.-m.; Zhang, C.-l.; Li, P. Characterization, Antimicrobial Activity, and Mechanism of a High-Performance (−)-Epigallocatechin-3-gallate (EGCG)−CuII/Polyvinyl Alcohol (PVA) Nanofibrous Membrane. *J. Agric. Food. Chem.* **2011**, *59* (9), 5087−5092.

(4) Ho, H.-Y.; Cheng, M.-L.; Weng, S.-F.; Leu, Y.-L.; Chiu, D. T.-Y. Antiviral Effect of Epigallocatechin Gallate on Enterovirus 71. *J. Agric. Food. Chem.* **2009**, *57* (14), 6140−6147.

(5) Hamza, A.; Zhan, C.-G. How Can (−)-Epigallocatechin Gallate from Green Tea Prevent HIV-1 Infection? Mechanistic Insights from Computational Modeling and the Implication for Rational Design of Anti-HIV-1 Entry Inhibitors. *J. Phys. Chem. B* **2006**, *110* (6), 2910−2917.

(6) Yu, H.-n.; Yin, J.-j.; Shen, S.-r. Growth Inhibition of Prostate Cancer Cells by Epigallocatechin Gallate in the Presence of Cu^{2+}. *J. Agric. Food. Chem.* **2004**, *52* (3), 462−466.

(7) Arimoto-Kobayashi, S.; Inada, N.; Sato, Y.; Sugiyama, C.; Okamoto, K.; Hayatsu, H.; Negishi, T. Inhibitory Effects of (−)-Epigallocatechin Gallate on the Mutation, DNA Strand Cleavage, and DNA Adduct Formation by Heterocyclic Amines. *J. Agric. Food. Chem.* **2003**, *51* (17), 5150−5153.

(8) Bursill, C. A.; Roach, P. D. Modulation of Cholesterol Metabolism by the Green Tea Polyphenol (−)-Epigallocatechin Gallate in Cultured Human Liver (HepG2) Cells. *J. Agric. Food. Chem.* **2006**, *54* (5), 1621−1626.

(9) Chen, Y.-K.; Cheung, C.; Reuhl, K. R.; Liu, A. B.; Lee, M.-J.; Lu, Y.-P.; Yang, C. S. Effects of Green Tea Polyphenol (−)-Epigallocatechin-3-gallate on Newly Developed High-Fat/Western-Style Diet-Induced Obesity and Metabolic Syndrome in Mice. *J. Agric. Food. Chem.* **2011**, *59* (21), 11862−11871.

(10) Walton, C.; Kalmar, J. M.; Cafarelli, E. Effect of caffeine on self-sustained firing in human motor units. *J. Physiol.* **2002**, *545* (2), 671−679.

(11) Biggs, S. N.; Smith, A.; Dorrian, J.; Reid, K.; Dawson, D.; van den Heuvel, C.; Baulk, S. Perception of simulated driving performance after sleep restriction and caffeine. *J. Psychosom. Res.* **2007**, *63* (6), 573−577.

(12) Carrier, J.; Fernandez-Bolanos, M.; Robillard, R.; Dumont, M.; Paquet, J.; Selmaoui, B.; Filipini, D. Effects of Caffeine are more Marked on Daytime Recovery Sleep than on Nocturnal Sleep. *Neuropsychopharmacology* **2007**, *32* (4), 964−972.

(13) Heatherley, S. V.; Hayward, R. C.; Seers, H. E.; Rogers, P. J. Cognitive and psychomotor performance, mood, and pressor effects of caffeine after 4, 6 and 8 h caffeine abstinence. *Psychopharmacology* **2005**, *178* (4), 461−470.

(14) Nawrot, P.; Jordan, S.; Eastwood, J.; Rotstein, J.; Hugenholtz, A.; Feeley, M. Effects of caffeine on human health. *Food Addit. Contam.* **2003**, *20* (1), 1−30.

(15) Luszczki, J.; Zuchora, M.; Sawicka, K.; Kozińska, J.; Czuczwar, S. Acute exposure to caffeine decreases the anticonvulsant action of ethosuximide, but not that of clonazepam, phenobarbital and valproate against pentetrazole-induced seizures in mice. *Pharmacol. Rep.* **2006**, *58* (5), 652−659.

(16) Ye, J.-H.; Liang, Y.-R.; Jin, J.; Liang, H.-L.; Du, Y.-Y.; Lu, J.-L.; Ye, Q.; Lin, C. Preparation of Partially Decaffeinated Instant Green Tea. *J. Agric. Food. Chem.* **2007**, *55* (9), 3498−3502.

(17) Perva-Uzunalić, A.; Škerget, M.; Knez, Ž.; Weinreich, B.; Otto, F.; Grüner, S. Extraction of active ingredients from green tea (Camellia sinensis): Extraction efficiency of major catechins and caffeine. *Food Chem.* **2006**, *96* (4), 597−605.

(18) Chang, C. J.; Chiu, K.-L.; Chen, Y.-L.; Chang, C.-Y. Separation of catechins from green tea using carbon dioxide extraction. *Food Chem.* **2000**, *68* (1), 109−113.

(19) Huang, K.-J.; Wu, J.-J.; Chiu, Y.-H.; Lai, C.-Y.; Chang, C.-M. J. Designed Polar Cosolvent-Modified Supercritical CO_2 Removing Caffeine from and Retaining Catechins in Green Tea Powder Using

Response Surface Methodology. *J. Agric. Food. Chem.* **2007**, *55* (22), 9014−9020.
(20) Liang, H.; Liang, Y.; Dong, J.; Lu, J.; Xu, H.; Wang, H. Decaffeination of fresh green tea leaf (Camellia sinensis) by hot water treatment. *Food Chem.* **2007**, *101* (4), 1451−1456.
(21) Beltrán, J. G.; Leask, R. L.; Brown, W. A. Activity and stability of caffeine demethylases found in Pseudomonas putida IF-3. *Biochem. Eng. J.* **2006**, *31* (1), 8−13.
(22) Kato, M.; Mizuno, K.; Crozier, A.; Fujimura, T.; Ashihara, H. Plant biotechnology: Caffeine synthase gene from tea leaves. *Nature* **2000**, *406* (6799), 956−957.
(23) Ogita, S.; Uefuji, H.; Yamaguchi, Y.; Koizumi, N.; Sano, H. RNA interference: Producing decaffeinated coffee plants. *Nature* **2003**, *423* (6942), 823−823.
(24) Sakanaka, S. A Novel Convenient Process To Obtain a Raw Decaffeinated Tea Polyphenol Fraction Using a Lignocellulose Column. *J. Agric. Food. Chem.* **2003**, *51* (10), 3140−3143.
(25) Ye, J. H.; Jin, J.; Liang, H. L.; Lu, J. L.; Du, Y. Y.; Zheng, X. Q.; Liang, Y. R. Using tea stalk lignocellulose as an adsorbent for separating decaffeinated tea catechins. *Bioresour. Technol.* **2009**, *100* (2), 622−628.
(26) Ye, J. H.; Dong, J. J.; Lu, J. L.; Zheng, X. Q.; Jin, J.; Chen, H.; Liang, Y. R. Effect of graft copolymerization of fir sawdust lignocellulose with N-vinylpyrrolidone on adsorption capacity to tea catechins. *Carbohydr. Polym.* **2010**, *81* (2), 441−447.
(27) Lu, J.-L.; Wu, M.-Y.; Yang, X.-L.; Dong, Z.-B.; Ye, J.-H.; Borthakur, D.; Sun, Q.-L.; Liang, Y.-R. Decaffeination of tea extracts by using poly(acrylamide-co-ethylene glycol dimethylacrylate) as adsorbent. *J. Food Eng.* **2010**, *97* (4), 555−562.
(28) Dong, Z.-B.; Liang, Y.-R.; Fan, F.-Y.; Ye, J.-H.; Zheng, X.-Q.; Lu, J.-L. Adsorption Behavior of the Catechins and Caffeine onto Polyvinylpolypyrrolidone. *J. Agric. Food. Chem.* **2011**, *59* (8), 4238−4247.
(29) Scordino, M.; Di Mauro, A.; Passerini, A.; Maccarone, E. Adsorption of Flavonoids on Resins: Cyanidin 3-Glucoside. *J. Agric. Food. Chem.* **2004**, *52* (7), 1965−1972.
(30) Liu, Y.; Liu, J.; Chen, X.; Liu, Y.; Di, D. Preparative separation and purification of lycopene from tomato skins extracts by macroporous adsorption resins. *Food Chem.* **2010**, *123* (4), 1027−1034.
(31) Lin, L.; Zhao, H.; Dong, Y.; Yang, B.; Zhao, M. Macroporous resin purification behavior of phenolics and rosmarinic acid from Rabdosia serra (MAXIM.) HARA leaf. *Food Chem.* **2012**, *130* (2), 417−424.
(32) Liu, Y.; Di, D.; Bai, Q.; Li, J.; Chen, Z.; Lou, S.; Ye, H. Preparative Separation and Purification of Rebaudioside A from Steviol Glycosides Using Mixed-Mode Macroporous Adsorption Resins. *J. Agric. Food. Chem.* **2011**, *59* (17), 9629−9636.
(33) Kammerer, D. R.; Carle, R.; Stanley, R. A.; Saleh, Z. S. Pilot-Scale Resin Adsorption as a Means To Recover and Fractionate Apple Polyphenols. *J. Agric. Food. Chem.* **2010**, *58* (11), 6787−6796.
(34) Chen, Z.; Zhang, A.; Li, J.; Dong, F.; Di, D.; Wu, Y. Study on the Adsorption Feature of Rutin Aqueous Solution on Macroporous Adsorption Resins. *J. Phys. Chem. B* **2010**, *114* (14), 4841−4853.
(35) Lou, S.; Chen, Z.; Liu, Y.; Ye, H.; Di, D. New Way to Analyze the Adsorption Behavior of Flavonoids on Macroporous Adsorption Resins Functionalized with Chloromethyl and Amino Groups. *Langmuir* **2011**, *27* (15), 9314−9326.
(36) He, C.; Huang, J.; Yan, C.; Liu, J.; Deng, L.; Huang, K. Adsorption behaviors of a novel carbonyl and hydroxyl groups modified hyper-cross-linked poly(styrene-co-divinylbenzene) resin for β-naphthol from aqueous solution. *J. Hazard. Mater.* **2010**, *180* (1−3), 634−639.
(37) Huang, J.; Wang, X.; Wang, X.; Huang, K. Hyper-cross-linked Polystyrene-co-divinylbenzene Resin Modified with Acetanilide: Synthesis, Structure, and Adsorptive Removal of Salicylic Acid from Aqueous Solution. *Ind. Eng. Chem. Res.* **2011**, *50* (5), 2891−2897.
(38) Li, H.; Jiao, Y.; Xu, M.; Shi, Z.; He, B. Thermodynamics aspect of tannin sorption on polymeric adsorbents. *Polymer* **2004**, *45* (1), 181−188.
(39) Avnir, D.; Jaroniec, M. An isotherm equation for adsorption on fractal surfaces of heterogeneous porous materials. *Langmuir* **1989**, *5* (6), 1431−1433.
(40) Sahouli, B.; Blacher, S.; Brouers, F. Applicability of the Fractal FHH Equation. *Langmuir* **1997**, *13* (16), 4391−4394.
(41) Jaroniec, M. Evaluation of the Fractal Dimension from a Single Adsorption Isotherm. *Langmuir* **1995**, *11* (6), 2316−2317.
(42) Calero, M.; Blázquez, G.; Martín-Lara, M. A. Kinetic Modeling of the Biosorption of Lead(II) from Aqueous Solutions by Solid Waste Resulting from the Olive Oil Production. *J. Chem. Eng. Data* **2011**, *56* (7), 3053−3060.
(43) El-Dissouky, A.; Elassar, A.-Z.; Bu-Olian, A.-H. Complex Formation, Metal Uptake, and Sorption Kinetics of a Chemically Modified Chlorosulfonated Polystyrene with Aminosalicylic Acid. *J. Chem. Eng. Data* **2011**, *56* (5), 1827−1839.
(44) Zhou, X.; Fan, J.; Li, N.; Qian, W.; Lin, X.; Wu, J.; Xiong, J.; Bai, J.; Ying, H. Adsorption Thermodynamics and Kinetics of Uridine 5′-Monophosphate on a Gel-Type Anion Exchange Resin. *Ind. Eng. Chem. Res.* **2011**, *50* (15), 9270−9279.
(45) Langmuir, I. The Adsorption of Gases on Plane Surfaces of Glass, Mica and Platinum. *J. Am. Chem. Soc.* **1918**, *40* (9), 1361−1403.
(46) Hu, X.; Wang, J.; Liu, Y.; Li, X.; Zeng, G.; Bao, Z.; Zeng, X.; Chen, A.; Long, F. Adsorption of chromium (VI) by ethylenediamine-modified cross-linked magnetic chitosan resin: Isotherms, kinetics and thermodynamics. *J. Hazard. Mater.* **2011**, *185* (1), 306−314.
(47) Kim, Y.; Kim, C.; Choi, I.; Rengaraj, S.; Yi, J. Arsenic Removal Using Mesoporous Alumina Prepared via a Templating Method. *Environ. Sci. Technol.* **2004**, *38* (3), 924−931.
(48) Saltalıa, K.; Sarıb, A.; Aydınc, M. Removal of ammonium ion from aqueous solution by natural Turkish (Yıldızeli) zeolite for environmental quality. *J. Hazard. Mater.* **2007**, *141* (1), 258−263.
(49) Baybaş, D.; Ulusoy, U. Polyacrylamide−clinoptilolite/Y-zeolite composites: Characterization and adsorptive features for terbium. *J. Hazard. Mater.* **2011**, *187* (1−3), 241−249.
(50) Ma, M.-H.; Lin, C.-I. Adsorption kinetics of β-carotene from soy oil using regenerated clay. *Sep. Purif. Technol.* **2004**, *39* (3), 201−209.